

# Impact of real case transmission systems constraints on wind power operation

François Vallée<sup>\*,†</sup>, Jacques Lobry and Olivier Deblecker

*Electrical Engineering Department, Université de Mons, Faculté Polytechnique, Boulevard Dolez, 31 B-7000 Mons, Belgium*

## SUMMARY

In this paper, a general strategy is proposed in order to introduce in a realistic way wind power into a HLII (bulk power system) nonsequential Monte Carlo adequacy study with economic dispatch. By use of the implemented solution, wind power can consequently be confronted to operational constraints related to high-powered thermal units, nuclear parks or cogeneration. Moreover, in order to optimize the large-scale integration of wind power production, the required reinforcements on a given electrical grid can also be evaluated on basis of the presented developments. The elaborated strategy can practically be applied to every kind of nonsequential Monte Carlo approach used to technically analyze a given transmission system. In the context of this work, the proposed solution has been implemented into the simulation tool Scanner<sup>©</sup> (property of Tractebel Engineering – Gaz de France – Suez company). Finally, in order to point out the efficiency and the usefulness of the proposed wind power model, the developed simulation tool has been firstly applied to an academic test system: the Roy Billinton test system (RBTS). Afterwards, in order to fully access the large offshore wind potential in the North Sea, the same tool has been used to evaluate the onshore reinforcements required in the Belgian transmission network. Copyright © 2010 John Wiley & Sons, Ltd.

KEY WORDS: transmission system; wind power; uncertainty; network reinforcement; investments; HLII reliability

## 1. INTRODUCTION

EACH investment scenario on a given electrical transmission system must ensure a quality service at the lowest cost (services continuity, system exploitation, behaviour when facing unexpected outage of a major element, . . .). In order to answer this major issue of modern networks, it is then necessary to compute a faithful representation of the transmission system. Therefore, a solution computing a large number of system states must be developed. In that way, statistical analysis by means of a Monte Carlo simulation [1–3] can precisely model the electrical system life by sampling a large set of representative states and consequently permit to obtain coherent exploitation cost and reliability indices for each studied network.

In a near future, stochastic electrical production and, more specially wind power, is expected to play an important role in power systems. Therefore, in order to capture the benefits of wind power, the rules and methods governing the planning and operation of the transmission network need to be optimized to take into account large-scale power production from wind farms and their locations. In that context, adequacy studies integrating wind power have been extensively developed for the HLI level (load covering with always available transmission system) [4,5]. From the bulk power system point of view, reliability studies taking into account transmission constraints have been introduced in order to evaluate reinforcements associated to large-scale wind farms integration [6,7]. However, those studies

<sup>\*</sup>Correspondence to: François Vallée, Electrical Engineering Department, Université de Mons, Faculté Polytechnique, Boulevard Dolez, 31 B-7000 Mons, Belgium.

<sup>†</sup>E-mail: francois.vallee@umons.ac.be

were conducted by use of a sequential Monte Carlo simulation and were thus requiring the use of large computer resources as the developed wind models were based on complex auto-regressive moving average (ARMA) time series [6,7]. Moreover, due to the inherent complexity of the sequential approach, those previous works were not considering eventual operational constraints (fatal production, nuclear or high powered thermal units that the producer does not want to stop during the nights ...) on classical generation units.

In the present study, as reliability and reinforcement analysis are long term studies, a general strategy is proposed in order to conveniently introduce wind power into a nonsequential Monte Carlo environment. By the use of such a Monte Carlo method, computing requirements are reduced without worsening the precision of the obtained global indices (indices of interest in the case of long term studies). Moreover, due to the greater simplicity of the developed models in the case of a nonsequential approach, HLII operating and transmission constraints can be simultaneously considered when facing an increased wind penetration. Therefore, it is believed that the proposed strategy will assist system planners and transmission system operators to qualitatively assess the system impact of wind power and to provide adequate input for the managerial decision process in presence of increased wind penetration. In that way, this strategy has been here implemented into the commercial software Scanner© (property of Tractebel Engineering – Gaz de France – Suez company) [8] but could have been applied to each kind of nonsequential Monte Carlo algorithm due to its generality. Finally, note that the goal of this work is not to study the short term balancing of wind uncertainty (with rapidly starting coal units) but rather to evaluate reinforcements and long term planning modifications to be made in order to improve and capture the benefits of wind power.

This paper is organized as follows. In a first part, the nonsequential Monte Carlo approach is presented in the context of HLII adequacy studies with economical analysis. Then, the methodology used to introduce wind power in such nonsequential environment is detailed. Thirdly, wind impact on reliability and reinforcement analysis for transmission systems is computed for an academic test system: the slightly modified RBTS [9]. In a Section 4, in order to fully access the large offshore wind potential in the North Sea, the developed simulation tool is used to point out the onshore reinforcements needed in the Belgian transmission network. Finally, a conclusion is drawn and summarizes the major results collected after the introduction of wind power into HLII analysis that takes into account operational and transmission constraints.

## 2. NONSEQUENTIAL MONTE CARLO SIMULATION IN THE CONTEXT OF HLII ADEQUACY STUDIES WITH ECONOMICAL ANALYSIS

### 2.1. System states generation

In this paper, the main objective of the nonsequential Monte Carlo simulation is to provide technical and economical analysis of development alternatives to be conducted on a given electrical transmission system (HLII approach). In that way, acceptance (or rejection) criterion is generally based on the following assessment: ‘Each investment scenario must ensure a quality service (system exploitation, healthy behaviour when facing unexpected outages, continuity of services ...) at the lowest cost’. In order to efficiently answer this issue, a complete analysis of the investigated system is needed. This requirement clearly points out the interest of using Monte Carlo simulations as those last ones model the system evolution as a set of static representative states. Practically, in order to generate the different system states, a nonsequential Monte Carlo algorithm generally loops on the 52 weeks of the year (Figure 1).

During each week, a given number (defined by the user according to the required accuracy on the calculated indices) of hourly system states can be generated by means of the following process:

- *Definition of the system state hour during the considered week:* Random generation by use of uniformly distributed numbers on the following fixed interval [0,168] (168 hours during a week);
- *For each generated hour:* Uniformly distributed random numbers ( $V$ ) on the interval [0,1] are sampled for each element (classical generation units, transformers, lines ...) in order to decide its operation state, using the following procedure [2]:

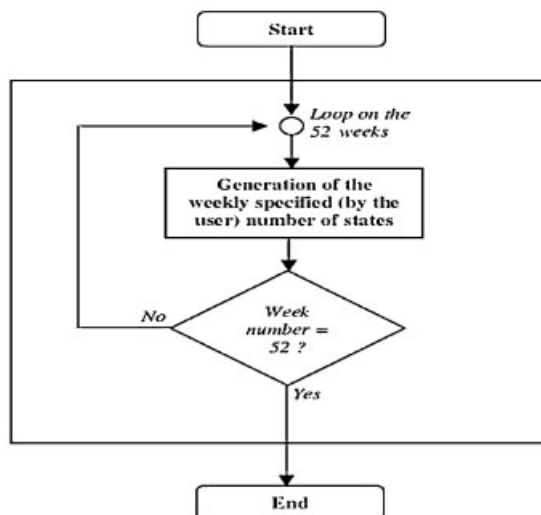


Figure 1. General algorithm of the system states generation process in a nonsequential Monte Carlo environment.

If  $V \leq$  forced outage rate (FOR that must be interpreted as a probability of unavailability), the element is considered as unavailable;

If  $V >$  FOR, the element is considered as fully available;

Note that, given the considered nonsequential environment, repair time [1] can not be explicitly defined for classical units. It must rather be implicitly taken into account in the FOR associated to those classical units. With that kind of approach, it is thus not possible to compute the duration of eventual load shedding states as a sequential approach would have permitted it. However, if the repair time is integrated in a global value of the FOR, it will also be possible to define states of load shedding in the nonsequential approach. Practically, those states will not appear sequentially as the nonsequential Monte Carlo simulation involves an independency between consecutively generated states. Nevertheless, at the entire simulation time scale and if the probabilities to be down were well defined for classical units, accurate global durations of load shedding can still be simulated with the proposed methodology (the only difference being that this global duration will not be obtained by a set of sequential hours or states but rather by the addition of nonsequentially defined load shedding states).

Concerning the hourly load at each node of the system, its determination in a nonsequential approach can be practically based on a random sampling over its cumulative distribution function [2] or, more precisely, established by the use of modulation diagrams of the annual peak load value [8]:

- *Diagram of weekly modulation of the annual peak load*: This last one permits to calculate the peak load of the current week on the basis of the annual peak load value for the considered node. This diagram contains thus 52 modulation rates of the annual peak load value.
- *Diagram of the hourly modulation of the weekly peak load*: It permits to calculate the hourly load for each hour of the week. This diagram contains thus 24 modulation rates of the weekly peak load value.

Using this last methodology, no random sampling is needed in order to generate the hourly load at each node of the system. More easily, the program just considers, in the weekly modulation diagram, the rate corresponding to the current week during the simulation process (Figure 1). Then, it associates to the generated weekly peak load the rate of the hourly modulation diagram corresponding to the investigated hour of the day. Also note that, as the consumption during 1 week can change from one day to the other (days of the week, Saturday or Sunday), several diagrams of hourly modulation can be associated to each node during one week. Moreover, seasonal aspects can also be taken into account by defining periods during the year and by changing the set of hourly modulation diagrams associated to each node from one period to the other.

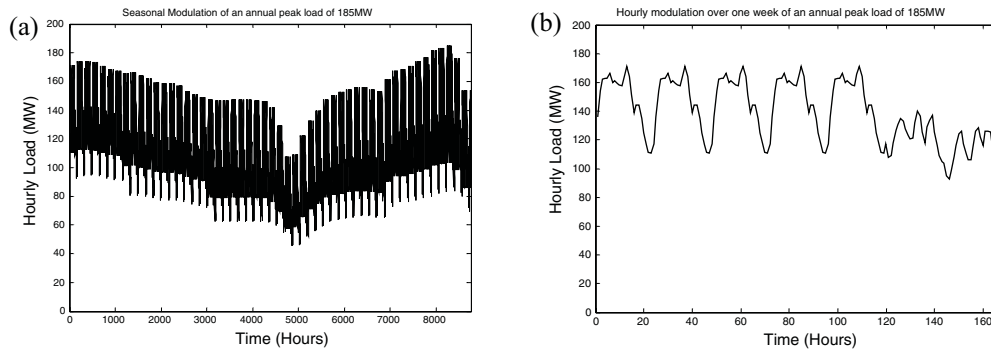


Figure 2. Seasonal modulation over one year for 185 MW peak load value (a) and hourly modulation over one week of the year for the same peak value (b) based on a Belgian real case [10].

Figure 2a illustrates the load behaviour during 1 year (based on a Belgian real case for the year 2000 [10]) for an annual peak load of 185 MW at the considered node. In Figure 2b, a zoom is made on one week of the year for the same node and illustrates the consideration of possible change of consumption from one day to the other inside the same week.

## 2.2. System states analysis

In order to efficiently estimate the investments and eventual reinforcements to be conducted on a given transmission system, each generated state must then be analyzed. This stage of the process can practically be achieved by use of three consecutive steps:

- (1) *Economic dispatch*: Generally based on the available production units and done *without considering transmission facilities availability*. The objective of this step is to ensure, at the lowest cost, the hourly load with the available production. Note that *an economic dispatch algorithm can take into account several possible constraints on classical units operation* like:
  - Hydraulic production and pumping stations: generally considered as a zero cost production (water is a cheap prime mover) and practically managed at a weekly time scale.
  - Thermal production: several types of constraints can be modelled for this kind of production. Firstly, *technical minima* (threshold under which the producer does not want to run its unit) can be considered for technical reasons like desired efficiency ... Secondly, units like cogeneration whose electrical production depends on an independent cycle (heat production) can be modelled using *forced units* that have a threshold over which they must always operate when they are available. Finally, in order to take into account high-powered thermal or nuclear units that the producer does not want to stop during the week, those machines can be considered as *long-term units* and must be managed at a weekly time scale. Practically, they have to run at least at their technical minimum value during the entire week when they are needed to cover all the reference peak consumptions of that week. Note that, when such a long-term unit is stopped during one week, it can not be started back before the start of the next week.

Finally, the algorithm that can be conducted during an economic dispatch with integration of operational constraints over conventional units proceeds as follows. In a first step, hydraulic production (cheap production cost) must be used to cover the load (following the orders of the weekly management). Then, technical minimum values of forced and long-term (if they are required to cover the reference peak loads during the week) thermal units are considered to satisfy the load (minus hydraulic production). Finally, an economic dispatch of the thermal production (minus the technical minimum values of already considered forced and long term units) is realized to cover the remaining load. Note that a disturbance reserve constraint can also be integrated in the economic dispatch resolution process. Practically, those reserves represent the fact that the transmission system operator wants to prevent consequences related to the loss

of the major unit of the production park. Generally, those reserves are constituted on basis of already started units or fast starting ones. It is commonly accepted that this reserve must be able to respond within 15 minutes after the production unit outage.

- (2) *Load flow*: When lot of system states are to be analyzed, load flows with alternative current hypothesis can lead to prohibitive computation times. Consequently, a DC load flow procedure can be more efficient to choose. Practically, this step carries out the computation of active power flows in transmission lines without considering reactive power and involves therefore several high voltage grid hypotheses: bus voltage magnitudes are close to 1 p.u., angular phase shifts between bus voltages are close to zero and line conductance is always negligible when it is compared to the susceptance.

In order to economically solve a DC load flow problem, generated active powers calculated during the economic dispatch must be introduced at the connection nodes of the concerned parks. Moreover, the generated hourly consumption for the current state must also be taken into account at the required nodes. DC load flow then computes active power flows over the transmission system and permits to take into account transmission links constraints. In case of line overflow, step 3 can eventually be started. On the opposite, if the optimal solution does not involve overloaded lines, this next step is avoided.

- (3) *Production rescheduling or load shedding*: This step is only useful if the optimal solution of the economic dispatch leads to overloaded lines during step 2. In that case, the solution is firstly 're-optimized' in order to avoid those unacceptable situations. Then, if this first stage is not sufficient to relieve all the overflows, an optimized load shedding procedure can be started in order to limit active power flows. Practically, the implemented algorithm tends to minimize the extra cost due to the eventual production rescheduling or load shedding under constraints like technical minimum power of classical units, power balance equations in buses, maximal power flows over transmission lines . . .

### 2.3. Calculated indices and productions

The most significant reliability indices that can be calculated during a technical analysis of a given transmission grid are certainly the loss of load expectation (LOLE in hours/year) [1] (HLI index calculated without considering transmission facilities) and the number of hours (per year) of load shedding (due to transmission overflows). Moreover, hours of overflows are also interesting to compute for each transmission line in order to point out the weakest points of the system.

Next to those indices, the annual production costs (with and without considering elements unavailability) can also be computed using the implementation of an economical analysis. Moreover, mean production and annual energy generated by each classical unit are also interesting to calculate. Finally, histograms of production can be printed out in order to analyze the utilization of each classical unit.

## 3. INTRODUCTION OF WIND POWER INTO AN HLII NONSEQUENTIAL MONTE CARLO TECHNICAL AND ECONOMICAL ANALYSIS

Due to the major increase of wind penetration in some countries (like Germany) [11], this variable kind of production can no more be neglected in technical and economical transmission system analysis. Therefore, in the present work, wind power has been implemented in such a nonsequential Monte Carlo simulation tool. In order to achieve that step, modifications related to the introduction of wind have to impact both major stages of the simulation process: *system states generation and the analysis of these states* (Sections 2.1 and 2.2).

### 3.1. Introduction of wind power in the system states generation process

Before taking into account wind power in the system states generation process, several entities related to wind power have to be defined. Those ones can be related to wind parks, wind speed regimes and power curves:

- *Wind parks*: Each wind park can practically be characterized by its installed capacity, production cost, FOR of one turbine, associated wind speed regime and power curve [12].

- *Wind speed regimes*: They are characterized by cumulative distribution functions (CDF) representing different statistical behaviours for wind speed in the investigated area. Those CDF can be classical *Weibull* distributions [12] or arbitrary ones. In the latter case, distributions can be linearly interpolated on the joint basis of a wind speed step and probability intervals defined by the user.
- *Power curves*: They transform wind speed into power. Practically, the conversion characteristics are linearly interpolated on the joint basis of the wind speed step and the power intervals defined by the user. An example of the linear interpolation related to a classical doubly fed asynchronous generation structure [13] is given in Figure 3. Note that a single conversion characteristic is practically applied to an entire park (worst case for reliability studies as it involves the most fluctuating production for a given wind park).

Once the different entities related to wind power have been defined by the user, the generation process can be started. The algorithm, executed when wind power is concerned, is presented in Figure 4. The applied methodology is the following one. During each generated system state, a first loop is started over the defined wind speed regimes and a wind speed per defined characteristic is generated by use of the classical inverse transform method [12]. By applying this methodology, it is supposed that wind parks subject to the same wind speed regime are entirely correlated. Based on Refs. [12,14], this approach will lead to the most fluctuating wind power and, thus, to the worst case for adequacy studies. Note that, here, as a nonsequential Monte Carlo approach is used, it is not necessary to use complex time series models for wind power [4–7]. Moreover, based on Ref. [15], in order to compute more realistic correlation coefficients of Pearson between different parks located inside the same cluster, an adequate normal noise can be defined by the user for each of those wind parks. This added distribution is then used to sample random contributions that are combined with the wind speed regime associated to the wind cluster in which the considered parks are located. Note however that this last methodology requires an adequate ‘user-implemented’ wind clustering methodology in order to yield (with a nonsequential Monte Carlo simulation tool) results close to the real behaviour of wind power over the studied territory [14,15].

Finally, a second loop is made over the defined wind farms. For each one, the associated wind speed is decided by taking the one sampled for the wind regime associated to the considered wind farm. Then, if the user wants to do so (need of accurate correlation between wind parks inside the same cluster), this wind speed can be combined with the user defined normal noise eventually associated to the considered wind park.

In the last step, each wind park production is calculated by introducing the sampled wind speeds in the associated power curves. Practically, power curves will be introduced in per unit and the real wind power (RWP) will be obtained by multiplying per unit quantities by the maximal available wind park capacity (MAWPC). The MAWPC can be related to the installed wind park capacity (IWPC) by approximation (1):

$$\text{MAWPC} = (1 - \text{FOR}) \text{IWPC} \tag{1}$$

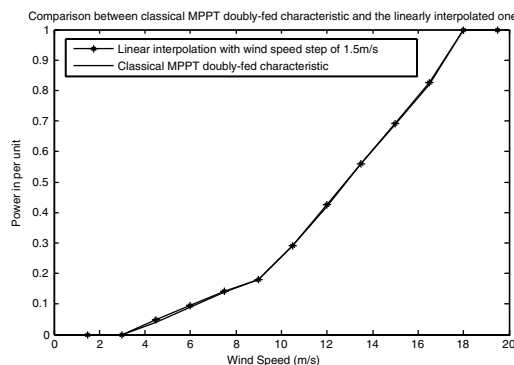


Figure 3. Comparison between classical maximum power point tracking (MPPT) power curve [13] and the linearly interpolated one (with a 1.5 m/s wind speed step) in per unit.

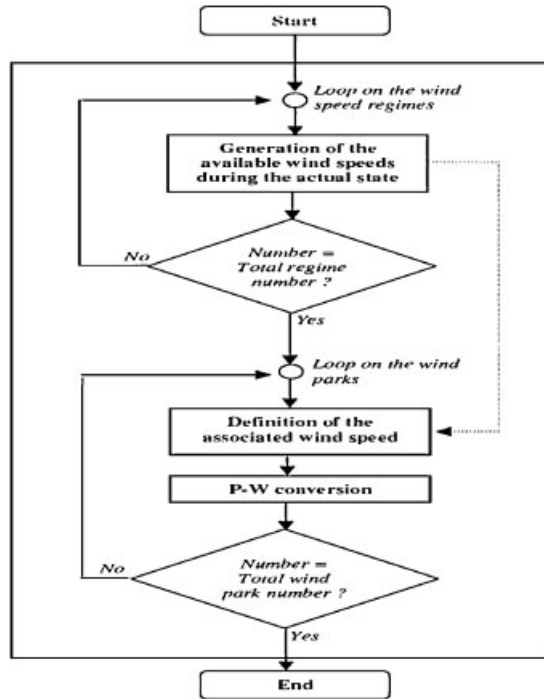


Figure 4. Algorithm of wind power sampling during each system state.

By applying (1), possible outages of wind turbines inside a park are *approached*. However, this hypothesis leads to acceptable results for high-powered wind parks connected to transmission systems as those last ones will be practically composed of a large number of turbines.

Alternatively, note that the state of each individual wind turbine can be more precisely defined by sampling uniform random numbers and comparing it to the turbine FOR (generalization of the sampling procedure used to define the state of each classical park; *cf.* Section 2.1 [1]). Finally, by adding the capacity of each available turbine, a more accurate value of MAWPC is obtained *via* this second method. Nevertheless, this approach is less immediate than the one based on Equation (1).

The described wind power sampling process must be started back for each system state. Consequently, a *Generated Wind Power Distribution* can be plotted at the end of the Monte Carlo simulation for each wind park '*i*'.

Figure 5 illustrates the obtained wind power distribution for one 8 MW wind farm subject to a *Weibull* wind speed regime (with scale parameter  $A = 9.25$  and shape parameter  $B = 2.15$ ) and using a maximum power point tracking (MPPT) power curve similar to the one depicted in Figure 3. Note that

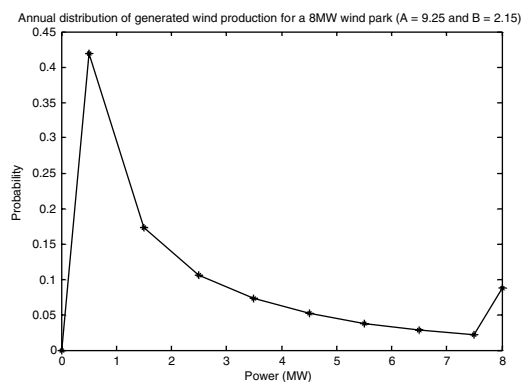


Figure 5. Simulated annual distribution of generated wind power for a 8 MW wind park ( $A = 9.25$  and  $B = 2.15$ ).

the increase of probability observed in Figure 5 near the installed capacity is due to the power limitation (at nominal power) usually applied in variable speed wind power units for wind speeds located between rated and cut out values [13].

### 3.2. Introduction of wind power in system states analysis

The generated wind power ( $GWP_i$ ) represents thus, for each defined park 'i', the sampled wind power during the simulated system state. This power must then be taken into account in the system state analysis.

The introduction of wind power into an economic dispatch algorithm has so been based on several starting hypotheses (return of experience):

- *Hypothesis 1*: It has been considered that wind power was not accurately predictable at the weekly time scale [11] and could therefore not impact the management of hydraulic and long term thermal (nuclear) units. Those classical units must thus be still processed at the weekly time scale without taking into account wind impact.
- *Hypothesis 2*: Wind power is considered as a must run production with zero cost. This hypothesis is based on the multiple encouraging policies that generally support wind power [16,17]. Consequently, in the economic dispatch, wind power will be directly considered *after* the technical constraints related to *forced and 'having to run' long-term thermal units*.
- *Hypothesis 3*: In case of increased wind penetration, the transmission system operator (TSO) can be forced (like it has already been the case in some German places [18]) to cut some wind power when facing conventional parks operating constraints [18]. In the proposed algorithm, when encountering such situations, wind power is decreased, for each wind park, proportionally to its available generated power.
- *Hypothesis 4*: As already mentioned in Section 2.2, dimensioning the disturbance reserve is commonly based on the largest unit tripping off instantaneously [19]. In that way, it can be considered [19] that wind power has no influence on the disturbance reserve as long as installed wind farms are less than the largest production unit in the system (which is still the case in the majority of countries). It has thus been supposed in this paper that the current wind penetration levels were not affecting the disturbance reserve. Concerning the short-term (several minutes) operational reserves used to balance wind power fluctuations, they are beyond the scope of this study (Section 1) as the investigated states are supposed to be steady-state hourly ones.
- *Hypothesis 5*: Concerning power quality and more specially voltage control with wind power, it is important to quote that the initial Scanner<sup>©</sup> algorithm is based on very high voltage ( $\geq 150$  kV) network hypotheses (Section 2.2). For very high voltage lines, their reactance  $X$  can practically be considered 10 times greater than their resistance  $R$  ( $X \geq 10R$ ) [20] and the classical expression (2) of the voltage drop in the line  $\Delta V$  can be simplified to (3) [20]:

$$\Delta V = \frac{RP + XQ}{V_2} \quad (2)$$

$$\Delta V = \frac{XQ}{V_2} \quad (3)$$

where,  $P$  and  $Q$  are, respectively, the active and reactive power flowing in the line,  $V_1$  and  $V_2$  the voltages, respectively, at generator and load connection nodes.

The active power generated by wind turbines is, by definition, highly fluctuating. By consequence, at the distribution level and based on Equation (2), it involves voltage fluctuations in the network area close to the connection nodes of wind turbines. In transmission grids with very high voltage lines, Equation (3) shows that voltage variations are essentially due to reactive power flows (on the opposite to distribution networks). Therefore, wind turbines currently connected to the transmission network must participate to the voltage control by means of a reactive power control. Given the recent developments in power electronics, this control is possible with the in-vogue doubly fed asynchronous or synchronous wind generators [20]. Based on those conclusions, it has been supposed in our developments that wind generators were able to entirely participate to the

voltage control and that the hypotheses related to the application of the DC load flow (bus voltage magnitudes are close to 1 p.u., angular phase shifts between bus voltages are close to zero; Section 2.2) were still applicable after the introduction of wind power in the Scanner<sup>©</sup> algorithm.

- *Hypothesis 6*: Stability aspects like transient stability, fault ride through capability, voltage flicker resulting from wind turbulence are of major importance when connecting a wind farm to the transmission grid. In that way, when assessing the wind farm stability, wind generators technologies (doubly fed induction wind generator, squirrel cage induction wind generator, converter-driven synchronous wind generator, directly coupled synchronous wind generator, . . .), wind conditions and the short circuit ratio ( $SCR = \text{short circuit power at the connection bus divided by the wind farm nominal power}$ ) at the point of common coupling (PCC) have a high importance. The SCR ratio can practically vary from very low values ( $SCR \approx 2$ ) that can be found in some remote areas in the USA or Australia [21] to higher values ( $SCR \geq 20$ ) for ‘strong networks’ like most of the European grids [21]. Refs. [21,22] propose a complete study of the combined impact of SCR and wind generator technology. In that way, it is shown that variable speed wind generators (DFIWG, CDSWG, DCSWG, . . .) provide a good transient stability in most cases (for both strong and weak networks), the only problematic situations coming from strong wind situations in some remote areas with a very low SCR. On the opposite, [22] clearly observes that wind farm stability with fixed speed wind generators (SCIWG) strongly depends on the short circuit power at the connection buses and that, in order to ensure a sufficient power quality, the SCR of the weakest buses must reach at least values greater than 20 with that kind of wind generators.

Power system reliability evaluation is an important part of various facilities planning, such as generation, transmission and distribution networks. Practically, power system reliability can be described by two important attributes: adequacy and security. Adequacy is the measure of a power system to satisfy the consumer demand in all steady state conditions and does therefore not include system disturbances. On the opposite, security is the measure of the system ability to withstand a sudden and severe disturbance while maintaining system integrity. Security is consequently associated with the system response to different disturbances and quantifies therefore stability aspects like transient stability or fault ride through capability . . . In this paper, the main objective of Scanner<sup>©</sup> is to provide a technical (and economical) analysis based on the *adequacy* evaluation of the investigated transmission system as each generated hourly state is supposed to be a steady one (Section 2.1). As a consequence, transient stability aspects are not under the scope of Scanner<sup>©</sup> and the impact of an eventual SCR increase (by an adequate planning of new power lines or by increasing the meshing of the transmission grid . . .) in order to improve the wind farm stability can not be evaluated with the Scanner<sup>©</sup> software.

The existence of some transmission system operation constraints can thus lead to a reduction of the real produced wind power. Therefore, in the developed algorithm, two quantities related to wind power have been defined *for each wind park*:

- Real wind power: It represents the real produced wind power after having taken into account the economic dispatch. A single  $RWP_i$  value is associated to each wind park ‘ $i$ ’;
- Lost wind power (LWP): It defines the difference between the generated wind power and the real produced one for each considered wind park. A single  $LWP_i$  value is thus calculated for each wind park ‘ $i$ ’.

The algorithm, implemented in order to take into account wind power in the economic dispatch associated to each generated system state, is described in Figure 6.

Based on hypotheses 1 and 2, wind power is thus used to cover the remaining load after that hydraulic production and technical minima of forced and ‘must run’ long term thermal parks (Section 2.2) have been taken into account. If this remaining load  $L_1$  is equal to zero, all the hourly load has already been covered before considering wind power. In that case, real transmitted wind power  $RWP_i$  is set to zero for each wind park ‘ $i$ ’ and their associated lost wind power  $LWP_i$  equals their initially  $GWP_i$  during the considered system state.

On the other hand, if the remaining load  $L_1$  is greater than zero, global generated wind power (GGWP) is taken into account before the remaining classical thermal production (without constraints)

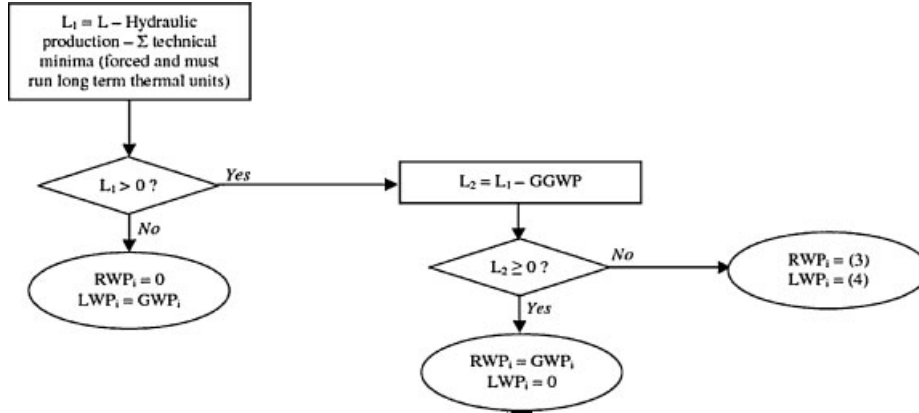


Figure 6. Algorithm implemented to take into account wind power for the economic dispatch of each generated system state.

and is entirely taken off from load  $L_1$ . If the obtained load value  $L_2$  (after consideration of hydraulic production, of forced and ‘must run’ long term thermal parks technical minima and of wind power) is greater or equal to zero,  $RWP_i$  equals the  $GWP_i$  for each park ‘ $i$ ’ and  $LWP_i$  is set to zero (and the classical economic dispatch is pursued). In the case of remaining load value  $L_2$  is negative, it is then necessary to reduce real transmitted wind power by following hypothesis 3. In order to apply this reduction of wind power, the remaining load  $L_1$  (before introduction of the generated wind power) is taken back. Parameters  $RWP_i$  and  $LWP_i$  associated to each defined wind park ‘ $i$ ’ are obtained on basis of Equations (4–6):

$$GGWP = \sum_{i=1}^N GWP_i \quad (4)$$

$$RWP_i = \frac{GWP_i \times L_1}{GGWP} \quad (5)$$

$$LWP_i = GWP_i - RWP_i \quad (6)$$

At the end of each system state economic dispatch,  $RWP_i$  and  $LWP_i$  values are thus defined for each wind park. In order to take into account wind power impact over transmission constraints, calculated  $RWP_i$  are then injected at the adequate nodes and the DC load Flow (Section 2.2) is launched. If no line overflows are recorded for the computed system state,  $RWP_i$  and  $LWP_i$  values remain unchanged for each wind park ‘ $i$ ’. On the opposite, in case of overloaded lines, the algorithm of rescheduling/load shedding (Section 2.2) is used and  $RWP_i$ ,  $LWP_i$  can have to be modified in order to ensure a safe behaviour of the transmission system.

The system state analysis leads thus now to the computation of  $RWP_i$  and  $LWP_i$  for each wind park ‘ $i$ ’. This process is set back for each generated system state. Consequently, at the end of the Monte Carlo simulation, histograms of  $GWP_i$ ,  $RWP_i$  and  $LWP_i$  can be drawn for each defined wind park ‘ $i$ ’. Moreover, mean values of generated ( $GWP_i$ ) and real ( $RWP_i$ ) exchanged wind powers are calculated for each wind park in order to point out the impact of transmission system constraints on wind power. Also note that reliability indices defined in Section 2.3 are now taking into account wind power.

#### 4. SIMULATION RESULTS ON A MODIFIED RBTS TEST SYSTEM

In order to point out wind power impact in transmission system management, a slightly modified version of the academic RBTS test system [9] has been considered (Figure 7).

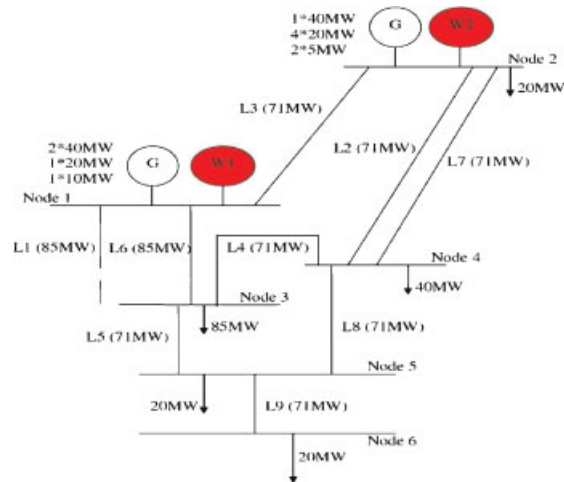


Figure 7. Implemented version of the RBTS.

In its initial version [9], the RBTS was not taking into account wind power. In order to introduce that renewable energy into the *RBTS*, Ref. [23] has consequently proposed the addition of wind power for an HLI adequacy study.

In this paper, the development is extended to the HLII hierarchical level. Indeed, the RBTS is slightly modified by connecting two wind parks at nodes 1 and 2 (Figure 7). Next to this small modification, transmission and classical production characteristics remain identical to those described in Ref. [9]. Finally, note that peak load is always 185 MW but that the weekly and hourly modulation diagrams have been based on the Belgian real case [10] given in Figure 2. Both considered wind parks are supposed to be located in distinct clusters. In that way, classical *Weibull* parameters for Belgian onshore ( $A = 8.1$  and  $B = 1.9$ ) and offshore ( $A = 10.6$  and  $B = 2.1$ ) sites have been considered [23]. At least, the same power curve is used for both parks and is based on the MPPT algorithm (Figure 3).

Compared to the initial version of the RBTS [9], operation constraints can be added, here, for classical parks (Section 2.2). In that way, two cases have been simulated:

- *Case 1*: No operation constraints are considered for the classical parks: all parks are supposed to be conventional ones without technical minimum value (and are neither forced nor long term ones).
- *Case 2*: Operation constraints are associated to the defined classical parks. Here, the sum of technical minima is supposed to be 75 MW. This value represents almost 30% of the installed classical capacity (240 MW) in reference to the Belgian real case [10]. Those 75 MW are divided in nuclear machines (30 MW), long-term thermal parks (30 MW) and cogeneration (15 MW).

Table I compares real transmitted mean wind power RWP with and without taking into account the operational constraints associated to conventional units. In that table, the given wind penetrations must be interpreted as a percentage of the installed conventional production (percentage of 240 MW). For example, it means thus that, when a 20% wind penetration is considered, the total (wind and conventional parks) installed capacity reaches  $240 + (0.2 \times 240) = 288$  MW. Based on the results of Table I, it can be clearly observed that technical constraints involve a reduction of the wind penetration (from 60 to 30%) at which the power initially available GWP cannot be entirely transmitted to the network (Figure 8). Moreover, at equivalent wind penetration and unchanged consumption characteristics, it can also be observed that operational constraints associated to classical parks lead to a more pronounced decrease of the real transmitted mean wind power RWP.

Practically, the impact of operational constraints mainly appears during light-load hours. Indeed, during those situations (usually occurring at nights), conventional units have been turned down to their maximum practical extent and wind curtailment is needed in order to assure system balance. For information, such difficulties of maintaining system balance under light-load conditions

Table I. Comparison between mean RWP transmitted to the RBTS network with and without classical unit operational constraints.

| Wind penetration (%) | RWPpark W1 (MW) with constraints | RWPpark W2 (MW) with constraints | RWPpark W1 (MW) without constraints | RWPpark W2 (MW) without constraints | GWPpark W1 (MW) | GWPpark W2 (MW) |
|----------------------|----------------------------------|----------------------------------|-------------------------------------|-------------------------------------|-----------------|-----------------|
| 0                    | 0.0                              | 0.0                              | 0.0                                 | 0.0                                 | 0.0             | 0.0             |
| 20                   | 7.0                              | 4.5                              | 7.0                                 | 4.5                                 | 7.0             | 4.5             |
| 30                   | 10.3                             | 6.7                              | 10.5                                | 6.8                                 | 10.5            | 6.8             |
| 40                   | 13.5                             | 8.8                              | 14.0                                | 9.1                                 | 14.0            | 9.1             |
| 50                   | 16.5                             | 10.7                             | 17.5                                | 11.3                                | 17.5            | 11.3            |
| 60                   | 19.1                             | 12.4                             | 20.9                                | 13.5                                | 21.0            | 13.6            |
| 70                   | 21.4                             | 14.0                             | 24.2                                | 15.6                                | 24.5            | 15.9            |
| 100                  | 26.8                             | 17.8                             | 33.2                                | 21.5                                | 35.0            | 22.7            |

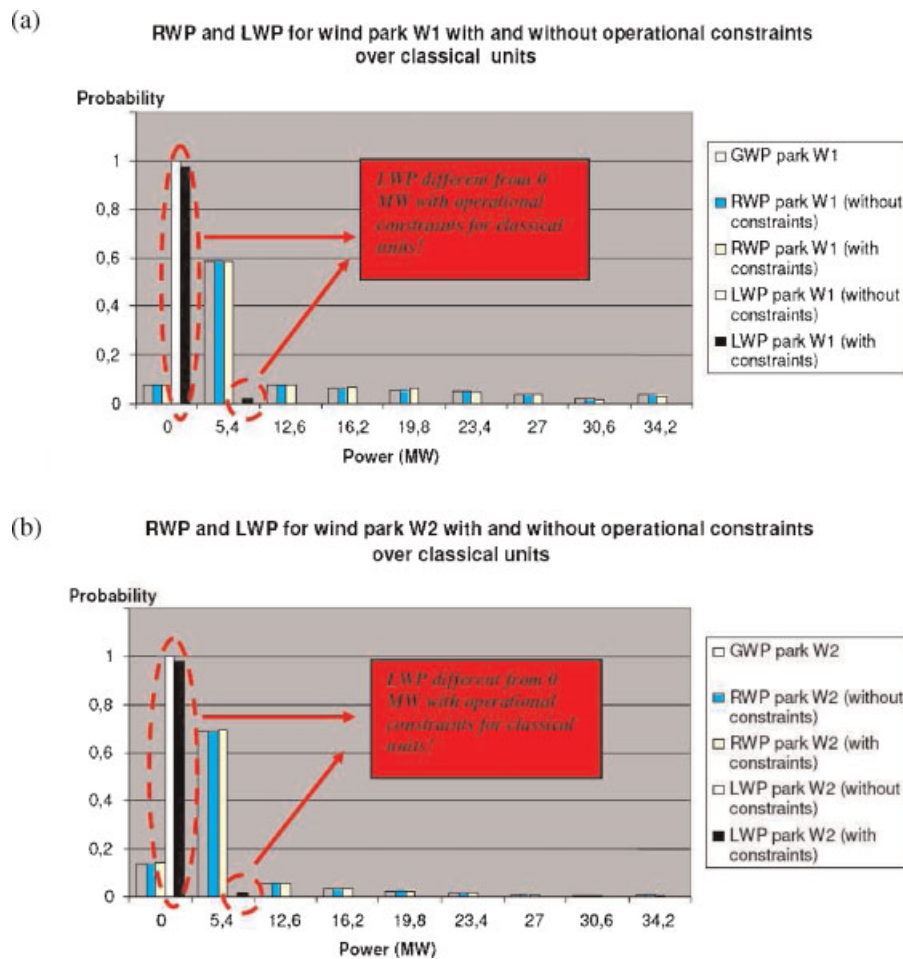


Figure 8. RWP and LWP (wind penetration of 30%) with and without taking into account operational constraints associated to classical units: results for wind park W1 (a) and W2 (b).

with significant wind variability have been recently put into relief in California, Canada [24] and Germany [18].

Finally, in order to point out a reduced impact of operational constraints under increased load conditions, the RBTS peak load value has then been increased from 185 to 240 MW (equally

Table II. Mean RWP and GWP for wind parks W1 and W2 with an increased peak load (240 MW).

| Wind penetration (%) | LOLE (hour/year) | Annual number of load shedding hours (hour/year) | RWP <sub>park</sub> W1 (MW) | GWP <sub>park</sub> W1 (MW) | RWP <sub>park</sub> W2 (MW) | GWP <sub>park</sub> W2 (MW) |
|----------------------|------------------|--|-----------------------------|-----------------------------|-----------------------------|-----------------------------|
| 0                    | 137.1            | 3.5 (node 3)                                     | 0.0                         | 0.0                         | 0.0                         | 0.0                         |
| 10                   | 102.6            | 3.1 (node 3)                                     | 3.5                         | 3.5                         | 2.3                         | 2.3                         |
| 20                   | 78.5             | 2.9 (node 3)                                     | 7.0                         | 7.0                         | 4.5                         | 4.5                         |
| 30                   | 61.3             | 2.8 (node 3)                                     | 10.5                        | 10.5                        | 6.8                         | 6.8                         |
| 40                   | 50.4             | 2.7 (node 3)                                     | 13.9                        | 14.0                        | 9.1                         | 9.1                         |
| 70                   | 30.4             | 2.5 (node 3)                                     | 23.1                        | 24.5                        | 15.0                        | 15.9                        |
| 100                  | 22.0             | 2.4 (node 3)                                     | 30.5                        | 35.0                        | 19.9                        | 22.7                        |

distributed between the five initial load nodes). In that case, the mean gap between operational constraints (unchanged) and light-load hours is increased. Therefore, an increased (from 30 to 40%) borderline wind penetration can also be logically observed in Table II. Nevertheless, if increasing the load improves the use of available wind energy under operational constraints related to conventional units, it implies larger power flows over the unchanged RBTS system. Consequently, in that scenario, it is not surprising to observe local load shedding situations at node 3 (Table II). Note that the wind penetrations given in Table II must again be interpreted as a percentage of the installed conventional production (percentage of 240 MW). Therefore, by increasing the wind penetration, the total (wind and conventional units) installed capacity is thus also increased which logically leads to reduced values of LOLE (as the load characteristics are unchanged for the different considered wind penetrations) in Table II. Moreover, the decreased number of load shedding hours, observed when wind penetration is increased, is explained by the fact that the complementary wind power installed at node 2 can be transmitted to sensitive node 3 without overloading the critic lines  $L_1$  and  $L_6$ . Consequently, when increasing the wind power installed at node 2, the number of load shedding hours at node 3 (due to overflows on line  $L_1$  or  $L_6$ ) is decreased.

The results proposed in this section point out the utility of the proposed models in order to improve the long-term management of wind power. Indeed, using this tool, transmission system operators will now be able to calculate the maximal wind penetration before meeting wind power decrease under light-load conditions.

## 5. INVESTMENTS STUDY FOR THE BELGIAN TRANSMISSION SYSTEM

In this paragraph, the proposed nonsequential Monte Carlo simulation tool is applied to the real case Belgian transmission system. As illustrated in Figure 9, this last one is highly interconnected and its topology can be practically explained by historical considerations. Indeed, along time, the voltage magnitude of the installed connections has been continuously increased from 36 towards 380 kV. Those new links have been systematically integrated in the already existing infrastructures and have consequently led to a highly interconnected Belgian transmission system. By the end 2007, the Belgian transmission network consisted so in 8406 km of high voltage links. The practical distribution of those lines is given in Table III and points out that the major part of the Belgian network is comprised between 70 and 150 kV [25].

In the early 2009, the installed production capacity connected to the Belgian transmission system was reaching 16.322 GW. This maximal power was practically produced by nuclear (6550.5 MW), thermal<sup>1</sup> (7914.6 MW) and cogeneration (692.9 MW) units. Also note that pumping stations are installed in Belgium for 1164 MW capacity. Concerning the Belgian consumption, the peak load value (considering the decentralized production connected to the distribution network) was about 14.033 GW by the end 2008 [26].

<sup>1</sup>Combined cycle units, coal thermal parks, diesel and turbo-jet units are included in this category.

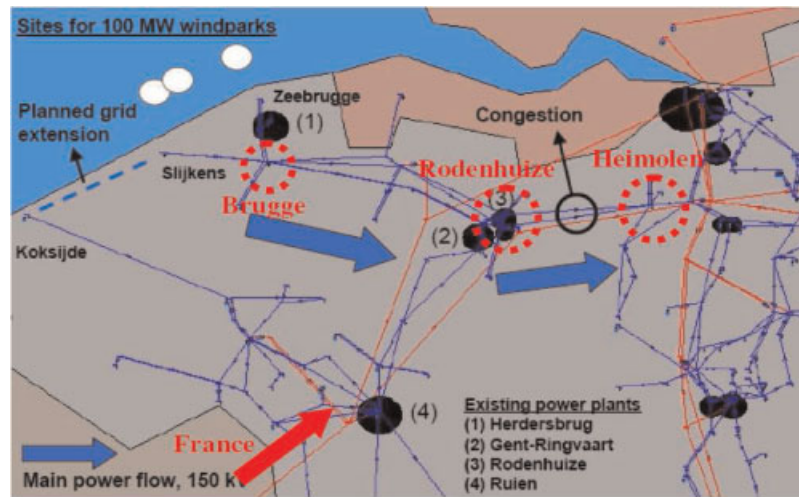


Figure 9. Major active power flows over the Belgian transmission system after large-scale integration of offshore wind power [27].

Table III. Electrical links in the Belgian transmission system by the end 2007 [25].

| Voltage magnitude (kV) | Underground cable (km) | Overhead line (km) | Total (km) |
|------------------------|------------------------|--------------------|------------|
| 380                    | —                      | 891                | 891        |
| 220                    | —                      | 297                | 297        |
| 150                    | 410                    | 2014               | 2424       |
| 70                     | 292                    | 2405               | 2697       |
| 36                     | 1922                   | 8                  | 1930       |
| 30                     | 141                    | 26                 | 167        |
| Total (km)             | 2765                   | 5641               | 8406       |

The major issue for the Belgian network concerns the optimal large-scale integration of offshore wind power. Indeed, by means of several deterministic load flows, Ref. [27] has firstly pointed out possible congestions between Rodenhuijze and Heimolen (Figure 9) if 100 MW offshore wind power were injected from Slijkens and Zeebrugge connection nodes and that 1 GW electrical power was simultaneously exchanged between France and the Netherlands. In the near future, two projects are going to be built in the North Sea for an installed wind capacity of 630 MW:

- *C-Power*: 60 wind turbines (5 MW) for an installed capacity of 300 MW (connection to the Slijkens 150 kV node).
- *Belwind*: 110 wind turbines (3 MW) for an installed capacity of 330 MW (connection to the Zeebrugge 150 kV node).

Those expected developments of offshore wind power clearly illustrate the need in investments studies in order to face this major challenge for the Belgian transmission system operator.

One of the interests of the proposed algorithm comes from the possibility to compute the annual number of hours with critic active power flow over the sensitive lines of the Flemish transmission system. In that way, Figure 10 clearly confirms that this number of critic hours increases with the installed offshore wind power for the Heimolen–Rodenhuijze 150 kV line. Further, it can also be observed that the 150 kV connections Slijkens–Brugge and Zeebrugge–Brugge do not undergo the large-scale offshore wind integration. This result is quite logical as the coastal transmission capacity was initially reaching 800 MW which is greater than the expected 630 MW installed wind power.

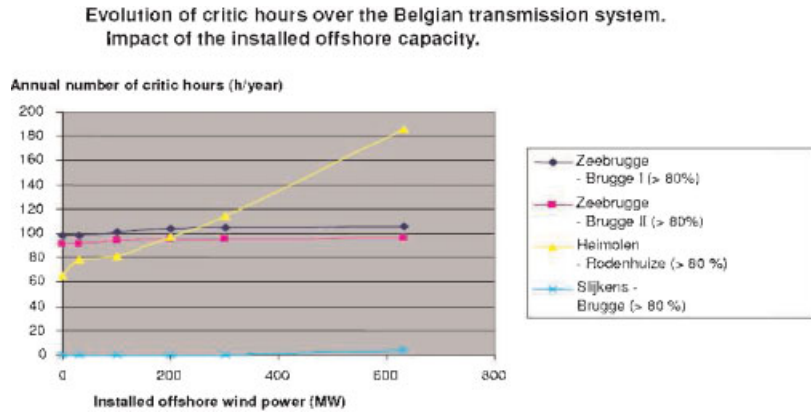


Figure 10. Critic hours (active power greater than 80% of line capacity) over major transmission lines in the Flemish high voltage system. Impact of the offshore wind power.

In order to improve the offshore wind integration and, consequently, to reduce the active power flows over the Rodenhulze–Heimolen line, the proposed solution has consisted in an additional 150 MW grid extension between Koksijde and Slijkens. Using this new line, simulation results (Figure 11) obtained with a 1 GW power exchange between France and the Netherlands point out a decrease of critic power flows on the Rodenhulze–Heimolen connection. This result can be easily explained as a fraction of the transmitted wind power is now deflected towards Koksijde.

However, after an increase to 2 GW of the electricity exchange between France and the Netherlands, a large decrease of the transmitted wind energy (Figure 12a) but also a dramatic increase of critic power flows between Rodenhulze and Heimolen (Figure 12b) can be observed with the developed simulation tool.

Consequently, in the context of largely interconnected European transmission systems, it will be imperative to imagine new reinforcements in the Belgian network. In that way, one of the possible solutions could come from the splitting of the Rodenhulze–Heimolen line. Indeed, in that case, Figure 13 shows a decrease of the simulated annual number of critic hours on this connection even if the power exchange between France and the Netherlands is set to 2 GW.

Finally, the previous simulation results clearly confirm the applicability of the proposed algorithm in order to evaluate reinforcements and long term planning modifications to improve and capture the benefits of wind power in transmission systems.

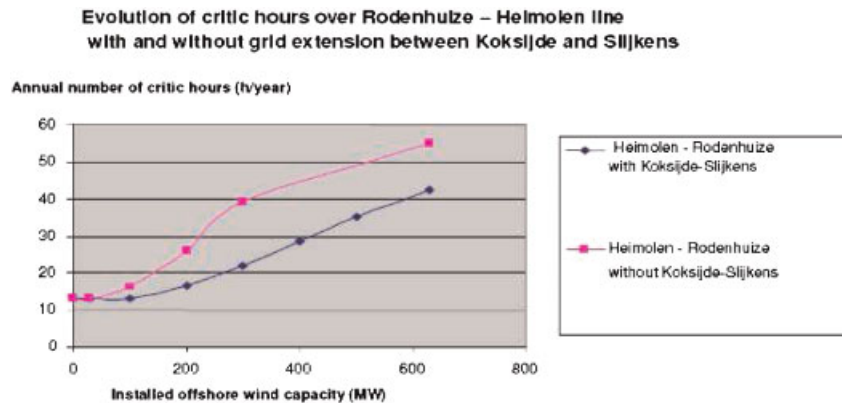


Figure 11. Critic hours (active power greater than 90% of line capacity) over Rodenhulze–Heimolen line with and without the added grid extension.

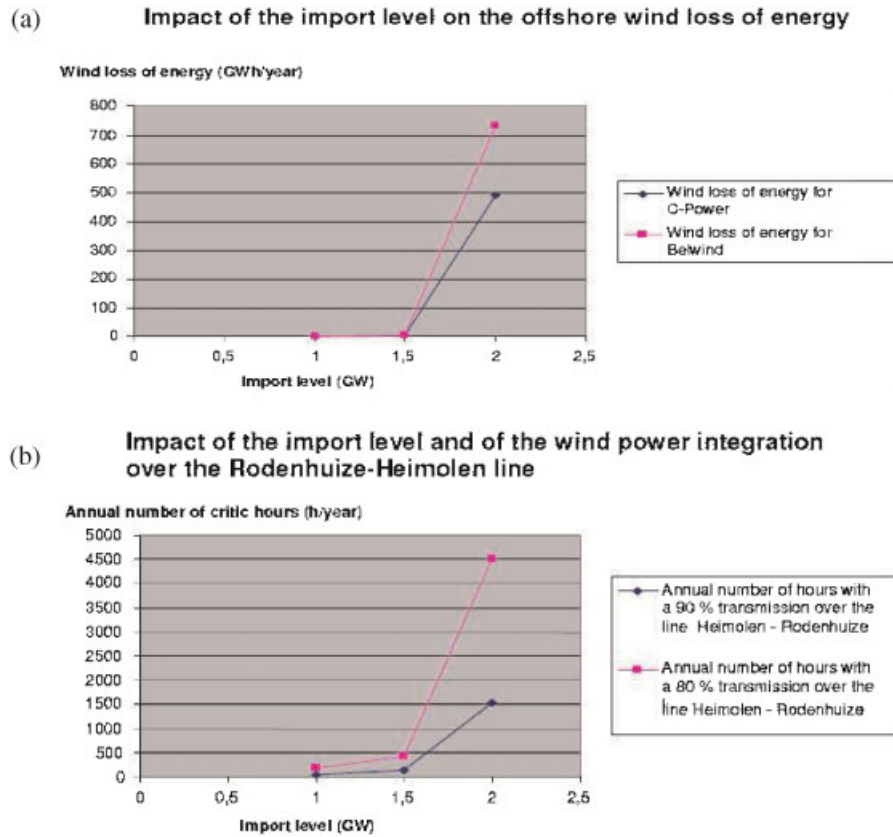


Figure 12. Impact of the import level between France and the Netherlands on the offshore wind loss of energy (a) and on the power flows between Rodenhuize and Heimolen (b).

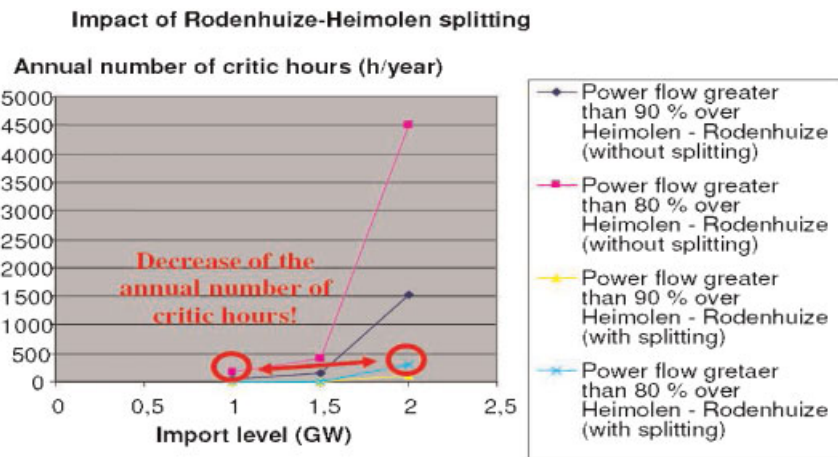


Figure 13. Impact of Rodenhuize–Heimolen splitting on critic power flows over the Belgian transmission system.

## 6. CONCLUSIONS

In this paper, wind power has been implemented into a transmission system technical and economical analysis. In that way, a general strategy has been proposed in order to conveniently implement wind power in a nonsequential Monte Carlo simulation tool that computes the investments to be conducted on a given transmission grid. Finally, a useful HLII analysis tool that takes into account wind power has

been developed and has permitted to study the impact of operational and power flow constraints over large-scale wind integration. In that way, situations of forced wind stopping were pointed out under operational constraints due to an increased wind penetration and light-load hours. Moreover, based on the proposed simulation tool, adequate reinforcements on the Belgian transmission system could also be evaluated in order to ensure an optimal integration of the expected offshore wind power. Finally, it is therefore believed that the proposed solution will assist system planners and transmission system operators to qualitatively assess the system impact of wind power and to provide adequate input for the managerial decision process in presence of increased wind penetration.

## 7. LIST OF ABBREVIATIONS

|       |   |
|-------|---|
| CDSWG | converter driven synchronous wind generator |
| DCSWG | directly coupled synchronous wind generator |
| DFIWG | doubly-fed induction wind generator         |
| FOR   | forced outage rate                          |
| GWP   | generated wind power                        |
| HLI   | hierarchical level I                        |
| HLII  | hierarchical level II                       |
| IWPC  | installed wind park capacity                |
| LOLE  | loss of load expectation                    |
| LWP   | lost wind power                             |
| MAWPC | maximal available wind park capacity        |
| PCC   | point of common coupling                    |
| RWP   | real wind power                             |
| SCR   | short circuit ratio                         |

## ACKNOWLEDGEMENTS

The authors gratefully acknowledge the contributions of S. Rapoport, K. Karoui and M. Stubbe from Tractebel Engineering – Gaz de France – Suez for the support given to this work.

## REFERENCES

1. Billinton R, Chen H, Ghajar R. A sequential simulation technique for adequacy evaluation of generating systems including wind energy. *IEEE Transactions on Energy Conversion* 1996; **11**(4): 728–734.
2. Papaefthymiou G, Schavemaker PH, Van der Sluis L, Kling WL, Kurowicka D, Cooke RM. Integration of stochastic generation in power systems. *International Journal of Electrical Power & Energy Systems* 2006; **18**(9): 655–667.
3. Bagen W, Billinton R. Incorporating well-being considerations in generating systems using energy storage. *IEEE Transactions on Energy Conversion* 2005; **20**(1): 225–230.
4. Billinton R, Bai G. Generating capacity adequacy associated with wind energy. *IEEE Transactions on Energy Conversion* 2004; **19**(3): 641–646.
5. Wangdee W, Billinton R. Considering load-carrying capability and wind speed correlation of WECS in generation adequacy assessment. *IEEE Transactions on Energy Conversion* 2006; **21**(3): 734–741.
6. Billinton R, Wangdee W. Reliability-based transmission reinforcement planning associated with large-scale wind farms. *IEEE Transactions on Power Systems* 2007; **22**(1): 34–41.
7. TradeWind Project. Integrating wind: developing Europe's power market for the large-scale integration of wind power, EWEA, Feb. 2009.
8. Scanner© Software. 1989; In-house developed software. Informations: [www.archives-suez.com/document/?f=presse/en/up1639.pdf](http://www.archives-suez.com/document/?f=presse/en/up1639.pdf).
9. Billinton R, Kumar S, Chowdhury N, *et al.* A reliability test system for educational purposes – basic data. *IEEE Transactions on Power Systems* 1989; **4**(3): 1238–1244.
10. Buyse H. Electrical energy production, Electrabel doc., available at: [www.lei.ucl.ac.be/~matagne/ELEC2753/SEM12/S12TRAN.PPT](http://www.lei.ucl.ac.be/~matagne/ELEC2753/SEM12/S12TRAN.PPT) 2004.
11. Ernst B. Wind power forecast for the German and Danish networks. In *Wind Power in Power Systems*, chapter 17, Ackerman Thomas (ed). John Wiley & Sons: Chichester, England, 2005; 365–381.

12. Vallee F, Lobry J, Deblecker O. System reliability assessment method for wind power integration. *IEEE Transactions on Power Systems* 2008; **23**(3): 1288–1297.
13. Al Aimani S. Modélisation de différentes technologies d'éoliennes intégrées à un réseau de distribution moyenne tension, Ph.D. Thesis, Ecole Centrale de Lille, chap.2, pp.24-25, December 2004.
14. Papaefthymiou G. Integration of stochastic generation in power systems, Ph.D. Thesis, Delft University, chapters 5 & 6, June 2006.
15. Vallee F, Lobry J, Deblecker O. Application and comparison of wind speed sampling methods for wind generation in reliability studies using non-sequential Monte Carlo simulations. *European Transactions on Electrical Power* 2009; **19**(7): 1002–1015.
16. Mackensen R, Lange B, Schlögl F. Integrating wind energy into public power supply systems – German state of the art. *International Journal of Distributed Energy Sources* 2007; **3**(4): pp.259-271.
17. Maupas F. Analyse des règles de gestion de la production éolienne : inter-comparaison de trois cas d'étude au Danemark, en Espagne et en Allemagne, Working paper, GRJM Conference, February 2006.
18. Sacharowitz S. Managing large amounts of wind generated power feed in – every day challenges for a German TSO and approaches for improvements. International Association for Energy Economics (IAEE), 2004 North American Conference, Washington DC, USA, 2004.
19. Holttinen H. The impact of large scale wind power production on the Nordic electricity system, Doctor of Science Thesis, Department of Electrical Engineering, Helsinki University of Technology, Finland, December 2004.
20. Robyns B, Davigny A, Saudemont C, *et al.* Impact de l'éolien sur le réseau de transport et la qualité de l'énergie, revue J3eA, vol. 5, Hors série no. 1, 2006.
21. Müller H, Pöller M, Basteck A, Tilscher A, Pfister J. Grid compatibility of variable speed wind turbines with directly coupled synchronous generator and hydro-dynamically controlled gearbox, 6th International Workshop on Large Scale Integration of Wind Power and Transmission Networks for Offshore Wind Farms, Delft, The Netherlands, 26–28 October, pp. 307–315, 2006.
22. Ledesma P, Usaola J, Rodriguez JL. Transient stability of a fixed speed wind farm. In *Renewable Energy*, vol. **28**, Elsevier Editions: United Kingdom, 2003; 1341–1355.
23. Raison B, Crappe M, Trecat J. Effets de la production décentralisée dans les réseaux électriques, Projet “Connaissances des émissions de CO2” Sous projet 5, FPMs, September 2001.
24. Smith JC, Thresher R, Zavadil R, *et al.* A mighty wind: integrating wind energy into the electric power system is already generating excitement. *IEEE Power & Energy Magazine March/April* 2009; 41–51.
25. Elia, Infrastructure management, Annual report 2007, pp. 18–19, January 2008.
26. Elia Memorandum Elia: Le gestionnaire du réseau de transport d'électricité en Belgique, Elia: l'énergie en bonne voie, pp. 5–17, 2009.
27. Van Roy P, Soens J, Driesen Y, Belmans R. Impact of offshore wind generation on the Belgian high voltage grid, European Wind Energy Conference (EWEC), Madrid, Spain, June 2003.